Hydrol. Earth Syst. Sci. Discuss., 9, 215–259, 2012
www.hydrol-earth-syst-sci-discuss.net/9/215/2012/
doi:10.5194/hessd-9-215-2012

Hydrology and Earth System Sciences Discussions

Water balance estimation in high Alpine terrain by combining distributed modeling and a neural network approach (Berchtesgaden Alps, Germany)

G. Kraller[1], M. Warscher[2], H. Kunstmann[2,3], S. Vogl[2,3], T. Marke[1], and U. Strasser[1]

[1]Institute for Geography and Regional Science, Karl-Franzens University of Graz, Heinrichstr. 36, 8010 Graz, Austria
[2]Karlsruhe Institute of Technology (KIT), Institute for Meteorology and Climate Change (IMK-IFU), Kreuzeckbahnstr. 19, 82457 Garmisch-Partenkirchen, Germany
[3]Institute for Geography, University of Augsburg, Universitaetsstr. 10, 86159 Augsburg, Germany

Received: 13 December 2011 – Accepted: 19 December 2011 – Published: 5 January 2012

Correspondence to: G. Kraller (gabriele.kraller@uni-graz.at)

Published by Copernicus Publications on behalf of the European Geosciences Union.

Abstract

The water balance in high Alpine regions is often characterized by significant variation of meteorological variables in space and time, a complex hydrogeological situation and steep gradients. The system is even more complex when the rock composition is dominated by soluble limestone, because unknown underground flow conditions and flow directions lead to unknown storage quantities. Reliable distributed modeling cannot be implemented by traditional approaches due to unknown storage processes at local and catchment scale. We present an artificial neural network extension of a distributed hydrological model (WaSiM-ETH) that allows to account for subsurface water transfer in a karstic environment. The extension was developed for the Alpine catchment of the river "Berchtesgadener Ache" (Berchtesgaden Alps, Germany), which is characterized by extreme topography and calcareous rocks. The model assumes porous conditions and does not account for karstic environments, resulting in systematic mismatch of modeled and measured runoff in discharge curves at the outlet points of neighboring high alpine sub-catchments. Various precipitation interpolation methods did not allow to explain systematic mismatches, and unknown subsurface hydrological processes were concluded as the underlying reason. We introduce a new method that allows to describe the unknown subsurface boundary fluxes, and account for them in the distributed model. This is achieved by an Artificial Neural Network approach (ANN), where three input variables are taken to calculate the unknown subsurface storage conditions. We explicitly derive the algebraic transfer function of an artificial neural net to calculate the missing boundary fluxes. The result of the ANN is then implemented in the groundwater module of the distributed model as boundary flux, and considered during the consecutive model process. The ANN was able to reproduce the observed water storage data sufficiently ($r^2 = 0.48$). The boundary influx in the sub-catchment improved the distributed model, as performance increased from NSE = 0.34 to NSE = 0.57. This combined approach allows distributed quantification of water balance components including subsurface water transfer.

1 Introduction

Alpine catchments are very important albeit vulnerable landscapes. Most of the major European rivers have their headwaters in Alpine catchments, and their discharge is transported via river systems to lower-lying areas (EEA, 2007). The Alps are crucial for water accumulation and water supply (e.g. Viviroli and Weingartner, 2004). For sustainable water management of water resources in alpine areas, it is imperative to understand the hydrological processes, their quantities and dynamics. Distributed hydrological modeling has become an important tool for describing the water balance in catchments (e.g. Goldscheider, 2011). However, those methods faces challenges in Alpine areas, on account of high altitudinal gradients, variation of meteorological parameters in time and scale, snow cover dynamics and unknown subsurface water fluxes and storages. The situation is even more complex, when the mountain ranges within a watershed consist of soluble limestone, dissected by small fractures and dominant flow paths up to caves and numerous spring locations, as is the case for this study area. The duality of karst, enfolding slow and fast infiltration, slow and fast groundwater flow and unknown storage, leads to heterogeneous water flow in the unsaturated and saturated zone (Attkinson, 1977; Bakalowicz, 2005; Kiraly, 2003; Sauter et al., 2006; White, 2002, 2003). Many approaches at different temporal and spatial scales deal with the modeling of hydrological processes in karst aquifers (e.g. Teutsch and Sauter, 1991). Spring hydrograph, chemograph, and tracer breakthrough curve analysis focus on small-scale effects of karst conduits to define the size and the characteristics of one individual spring aquifer (Birk et al., 2004; Einsiedl, 2005; Geyer et al., 2008; Bonacci, 2004; Hauns et al., 2001; Kovacs et al., 2001; Grasso and Jeannin, 2002; Maloszweski et al., 2005; Weiler et al., 2003). Other approaches concentrate on karst genesis or theoretical conduit flow (Sauter et al., 2006; Romanov et al., 2004; Ford, 2003). Distributive methods, such as “Single Continuum Porous Equivalent”, “Double Continuum Porous Equivalent”, “Discrete Single Fracture Sets” or “Discrete Multiple Fracture Set”, “Hybrid Models” (Sauter et al., 2006) attempt to take into account the heterogeneity of

karst aquifers within single conduits or parameter fields in a spatial continuum, however mainly concentrate on modeling water fluxes within the saturated zone. The duality of karst makes it tremendously difficult to find an adequate parameterization to successfully model groundwater flow in present distributed models, which principally assume porous conditions (Kiraly, 2003). In the past, many studies have applied distributed groundwater models in karst environments (Scanlon et al., 2003; Caroll et al., 2008; Martinez Santos and Andreu, 2010; Worthington, 2003), or other conceptual approaches such as (Rimmer and Salingar, 2006). These approaches do not deal with the effects of a massif Alpine karst aquifer itself on the hydrology of a catchment or sub-catchment. Barthel (2011) recommends groundwater studies that focus on the catchment scale. Kunstmann et al. (2006b) applied the distributed model WaSiM-ETH in alpine catchments. To the author’s knowledge, so far, no attempt has been made to examine the complete water balance of an Alpine karstified watershed and its subcatchments by applying a distributed hydrological model to determine possible subsurface boundary fluxes. White and White (2003) describe groundwater basins as total recharge areas including all surface stream catchments that drain into the conduit system of a spring. Overall, karst ground water basins from springs do not correlate with the boundaries of overlying surface water basins; they may also be linked by piracy or spillover routes. Conduits develop across surface water divides thereby transmitting water to or from other nearby surface water basins. Furthermore, groundwater basins have one set of flow paths active during base flow conditions and quite a different set of flow paths during flood flow conditions (White and White, 2003). Our study area is characterized by hundreds of springs connected to fracture, conduit or cave systems with an unknown set of active or inactive flow paths. We assume, however, that water fluxes in an high Alpine 1000 m banked limestone aquifer with an inclined stratification can lead to groundwater inflow, outflow or redistribution on an even larger scale than spring basins – at catchment scale, where subbasins cover valleys in mountainous regions, and that this affects river runoff within those subbasins and consecutive streams.

Summary of the new approach

Within the study area, each of the three high Alpine head subcatchments is unique in subsurface hydrological systems (Kraller et al., 2011), and measured runoff differs significantly in between the valleys within the same time period. By applying the distributed model, we are able to show that high Alpine aquifers do have tremendous effect on the hydrology of subbasins and that common approaches for distributed modeling (Richards, 2-D – Groundwater-Model, Darcy and continuity equation) of water balance perform insufficiently. By analyzing measured runoff, and model results for precipitation, evapotranspiration and runoff we found systematic data patterns in model mismatch, and, consequently mismatch in modeled and observed water storage in three neighbouring subbasins "Klausbachtal", "Wimbach" and "Königsseetal" (Fig. 1). This under- and overestimation affects model results in consecutive subbasins within the model area and the model area outflow. Different precipitation interpolation approaches did not allow to correct for this mismatch. Therefore, we conclude that different storage conditions lead to under and overestimation of runoff, and thus we develop a method to calculate missing water fluxes to enable flexible inflow and outflow at subbasin scale on a monthly time basis. We derive the analytical solution of the artificial neural net to calculate observed water storage which can be implemented in the distributed model as inflow or outflow in the saturated zone as continuous boundary flux (Fig. 2). The implemented flux is considered in the model run and affects modeled stream discharge of consecutive subbasins. Not only does this method allow to describe water storage dynamics and resulting groundwater inflow and outflow in karstic terrains; it also allows to adapt distributed hydrological models to karst dominated watersheds.

2 Study area and former karst research results

The study site encompasses the watershed of the river Berchtesgadener Ache and is situated in the Berchtesgaden Alps in the southeast of Germany in the Federal State of

Bavaria. The area covers 432 km^2 and is mostly German territory. Ten per cent, however, is Austrian national territory. Most of the area can be assigned to the *Man and Biosphere Reserve Berchtesgaden*, of which the core zone is Berchtesgaden National Park (IUCN Category II) with an area of 210 km^2 (Fig. 1). The climate in the area is cool-temperate and humid. Mean temperature is 4.5 °C. Precipitation has an altitude – dependent gradient of 47 mm/100 m. Annual precipitation ranges from 1500 mm in the valleys to up to 2600 mm in higher elevated regions. Maximum precipitation is 250–350 mm in July in the high Alpine regions of the test site, albeit high uncertainties exist as only few stations are established in higher regions. The number of days with snow cover is more than 300 per year in peak regions. Dominant biotopes are forest, limestone grasslands, rock and scree, mountain pines and lakes and glaciers. The Berchtesgaden Alps are situated in the northern limestone Alps and can be seen as a geomorphological unit. The nine associated mountain ranges to the watershed "Berchtesgadener Ache" are shaped in close proximity as plateaus and ridges. Three valleys stretching from south to north, separating four mountain massifs from each other are representative for the area. Dominant rock formations are Triassic Dachstein limestone and Ramsau Dolomite, but Jurassic and Cretaceous rock series are also present. The banked limestone with a layer thickness of up to 1000 m covering 500–700 m of Dolomite extends along an altitudinal gradient up to 2100 m (Fig. 3). The three main tectonic units in the area are arranged on top of one another: The base Tirolikum is covered by the Tiefjuvavikum which itself lies beneath the Hochjuvavikum. Alpine fold leads to a typical slope and inclined stratigraphy of the existing rock formations. The mountain massifs Hochkalter and Watzmann slope slightly in a northern direction (Fischer, 2005; Langenscheidt, 1994). The soluble limestone has been exposed to karstification processes since the Alpine lift, which took place in different phases. Typical karst phenomena in the region are the presence of dolines, basins, dry stream beds, caves and karrens. The massif karst aquifer in the area is characterized by matrix, fractures and conduits. The epikarst and vadose zones are more dominant than the phreatic zone. Most of the spring discharge is a reaction to precipitation events.

A spring horizon at the south shore of a lake which shows phreatic behaviour but reacts also to precitpitation events. There are no permanent sinking streams within the study area, but snowmelt and rain immediately infiltrate through swallow holes, especially on karst plateaus. Based on spring locations, the boundary between unsaturated and saturated zone is estimated at an altitude of 601 m a.s.l. and 1500 m a.s.l. maximum, but mainly at 700–1000 m a.s.l. Consequently, the unsaturated zone can be up to 1000 m in thickness. The eight rivers within the watershed drain the area in a northerly direction. Based on nine river gauges available for the basin, it can be divided into nine subbasins (Fig. 1). Several tracer experiments, a spring database and geological conditions indicate a main groundwater flow direction from the south. Furthermore, groundwater redistribution between subcatchments is also indicated between three neighbouring Alpine head sub-catchments streching from north to south (Kraller et al., 2011). These subbasins are located in a highly karstified area with a steep terrain. Subbasin Klausbachtal (42.79 km^2) is characterized by forests at lower altitudes and high Alpine plateau and ridge karst at higher altitudes. It is bounded by the plateau mountain Reiteralm and mount Hochkalter. Subbasin Wimbachtal (35.69 km^2) is filled with Dolomite gravel deposits, forming a porous aquifer with a depth of 300 m. It is surrounded by mounts Hochkalter and Watzmann, which are characterzied by a huge carbonate stratum. In the southern part, it is surrounded by dolomite mountains. Subbasin Königsseetal (163.54 km^2) is characterized by Lake Königssee (511 mio m^3) and very steep gradients. It is bounded by mount Watzmann and the Hagengebirge plateau, while to the south it is surrounded by a huge Alpine karst plateau, called "Steinernes Meer". Geologically and hydrologically, these neighboring subbasins show unique geological and hydrological features (Fig. 3).

3 Distributed modeling in high Alpine terrain

3.1 Model set up

We applied the distributed model WaSiM-ETH (Schulla, 1997, 2007) in a horizontal resolution of 50 m and a temporal resolution of 1 h. The basin and borders of the subbasins were derived by the digital elevation model and the location of river gauges. Eight gauges are located in Germany and one in Austria. The model uses physically-based algorithms within its modular system. Precipitation interpolation was done using Inverse Distance Weighting and linear regression linearly combined (IDW weighted with 0.25). Interpolation of other meteorological input data was done by Inverse Distance Weighting. Infiltration is calculated after Peschke (1977), evapotranspiration after Penman-Monteith (Penman, 1948; Monteith, 1975; Brutsaert, 1982), snow cover dynamics are calculated following Strasser (2008). Direct flow (surface runoff) is the sum of infiltration excess, saturation excess and a defined fraction of the snow melt. Vertical soil water fluxes within a defined number of soil layers and depth in the unsaturated zone are described by solving the Richards equation (Richards, 1931). Soil parameterization is done according to Van Genuchten (1976). Interflow is calculated depending on suction, drainable water content and saturated hydraulic conductivity. The distributed model was applied with a 2-D groundwater model coupled to the unsaturated zone with a vertical boundary flux. The lower boundary of the unsaturated zone is the depth of the groundwater layer. Horizontal groundwater flow is calculated by the flow equation derived from Darcy's law and the continuity equation. The saturated zone is located within the defined soil layers and depth, groundwater level is calculated corresponding to soil water content and previous storage conditions. The aquifer is assumed to be unconfined. Storage conditions within the unsaturated zone are initialized for each discretization layer with a water content corresponding to an hydraulic equilibrium with the groundwater (fluxes are zero) and the groundwater table is assumed to be at a depth of 20 % of the soil column. In principle, the model environment is not able to account for karstic underground. A porous aquifer is assumed. It

represents a substitutional porous media model whose parameters must be interpreted as effective parameters approximating the karstic environment on subcatchment scale (Kunstmann et al., 2006a). Next to numerous free model parameters, sensitive calibration parameters are the recession constant k_{rec} for the saturated hydraulic conductivity and the interflow drainage density d_r (Schulla, 1997, 2007). Discharge routing is done with a kinematic wave approach, including a flow time table, retardation and translation. Due to fast infiltration and high evapotranspiration in bare karst area, we adapted parameters for evapotranspiration over rock surfaces leading to increased evapotranspiration for these areas. Furthermore, we also allowed for macropore – infiltration as it is implemented in the distributed model after Jansson and Karlberg (2001). Data for soil classification were derived from the existing soil database of the National Park authority and the concept soil map provided by the Bavarian Environment Agency. Land use classification was derived from Lotz (2006) and Corine Land Cover data. We classified 15 land use types and 20 soil types within the model area. Soil stratification was defined for 40 layers with a depth of 0.2 m to 4.0 m according the distributed porous approach. Information on the hydraulic saturated conductivity was derived from BGRSGD (2007). Best parameterization for aquifer thickness and the specific storage coeffcient were iteratively estimated. River courses were derived from the digital elevation model during preprocessing. The discharge data was provided by the Traunstein water management office and the Salzburg hydrographical service. Meteorological input data was provided by 33 weather stations whereby 20 are automatic and 15 are mechanical stations (Table 1). The stations are equally distributed in altitude (604–1973 m a.s.l.) and space throughout the model area (Fig. 4)

3.2 Analysis of precipitation interpolation methods

We found, there to be a mass problem within the distributed model, because it was not able to reproduce measured runoff in the Alpine head catchments. Various interpolation methods to analyze whether precipitation input data was the cause for the deviation or not were investigated. The precipitation interpolation methods Inverse Distance

Weighting (IDW), Elevation Dependent Regression and a linear combination of IDW and Elevation Dependent Regression (weighting factor IDW: 0.25) were tested for the annual sum of precipitation in subbasin Königsseetal. Annual sums of interpolated precipitation were 1559 mm for IDW, 1704 mm for regression and 1643 mm for the linear combination of both methods (Table 2). IDW shows the lowest value because the elevation dependency of the precipitation was not considered (1559 mm). Analyses of station data within the area however proved gradient dependency of precipitation amount. In high Alpine terrain, IDW was not considered appropriate for the application. Regression showed the highest value, because it did not reproduce station data (1704 mm). The combined method is giving a value between the two other methods, because it takes into account elevation dependency and station data (1643 mm). We analyzed both methods for one station by comparing the overall mean from 2001–2010. The analysis revealed that REG + IDW could best reproduce the station data. Figure 5 shows modeled runoff resulting from the different interpolation methods. Runoff dynamics differ slightly, and no method resulted in improved model results. Therefore, we conclude unknown storage processes to be the most likely cause for the model mismatch.

3.3 Outcomes distributed modeling – identification and quantification of boundary fluxes

In a first step, we analyzed annual sums and overall means of measured runoff and modeled precipitation, evapotranspiration and runoff at the river gauges of the three high Alpine neighbouring head subbasins Klausbachtal (1), Wimbachtal (2) and Königsseetal (4) (Table 3). Annual sums of measured runoff ranged from 996 mm to 1375 mm in subbasin Klausbachtal (mean 1207), from 1045 to 2808 mm in subbasin Wimbachtal (mean 2091) and from 1197 to 1831 mm (mean 1604) in subbasin Königsseetal. Annual sums of measured runoff differed significantly in these subcatchments. Precipitation ranged from 1607 to 2112 mm in subbasin Klausbachtal, from 1621 to 1940 mm in subbasin Wimbachtal and from 1511 to 1869 mm in subbasin

Königsseetal, resulting in an overall mean of 1772 mm (Klausbachtal), 1704 mm (Wimbachtal) and 1681 mm (Königsseetal), respectively. Mean annual evapotranspiration was 367 mm for subbasin Klausbachtal, 348 mm for subbasin Wimbachtal and 425 mm for subbasin Königsseetal. The measured runoff indicates a unique hydrology in each valley. After distributed model calibration, model runs result in equally calculated annual sums of modeled runoff, dependent on precipiation input. Mean annual modeled discharge was 1325 mm in subbasin Klausbachtal, 1280 mm in subbasin Wimbachtal and 1201 mm in subbasin Königsseetal. Consequently, a systematic over- and underestimation of discharge was found in these sub-catchments when comparing modeled to measured runoff (Fig. 6). Based on analyses of several precipitation interpolation approaches, we assume that different annual sums of measured runoff in subbasin Klausbachtal, Wimbachtal and Königsseetal to be the result of subsurface boundary fluxes that were not taken into account by the distributed model, leading to under and overestimation of measured runoff during model runs. Since it is the characteristic subsurface conditions and resulting water fluxes that influence the water balance in karst aquifers, the monthly sums of water storage for subbasins Klausbachtal, Wimbachtal and Königsseetal were analyzed in model runs and reality to gain more information about the annual dynamics of the water storage. By substracting the runoff (Q) from the incoming effective precipitation (Eq. 1) storage reduction or buildup is expressed and is assumed to be positive in winter and summer (snow storage and soil storage) and negative in spring and autumn (snow melt and soil storage decrease), leading to a systematic pattern throughout one year. Deviations from the assumed pattern for the observed water storage may give insights into groundwater inflow, outflow or redistribution at subbasin scale due to subsurface water fluxes. Monthly sums of modeled and observed water storage were analyzed (Eqs. 2 and 3).

$$P_{\text{eff}}(t) = P(t) - \text{ET}(t) \quad (1)$$

$$S_{\text{mod}}(t) = P_{\text{eff}}(t) - Q_{\text{mod}}(t) \quad (2)$$

$$S_{\text{obs}_{\text{real}}}(t) = P_{\text{eff}}(t) - Q_{\text{meas}}(t) \quad (3)$$

Figure 7 a shows the water storage modeled for the subcatchments Klausbachtal, Wimbachtal and Königsseetal in monthly sums for the summer period in years 2001 to 2011. Storage is always positive as there is less runoff than precipitation income (soil storage buildup) in the distributed model. The monthly sums of modeled runoff show positive values. Figure 7b shows the water storage derived from the measured runoff. It shows negative peaks during summer for subbasins Klausbachtal and Königsseetal (Fig. 7b). There is more runoff than precipitation coming in, indicating groundwater inflow and explaining the amount of measured annual runoff. In subbasin Klausbachtal, there is less soil storage and snow melt, indicating groundwater outflow and explaining the annual lack of water. Table 4 shows the maximum, minimum and mean of monthly modeled and measured water storage. In subbasin Klausbachtal, mean of observed water storage is positive (15 mm), indicating water outflow from the subbasin. It is underestimated by the distributed model (−2 mm), because water outflow is not calculated and all incoming precipitation is routed to the stream. In subbasins Wimbachtal and Königsseetal, mean water storage is negative (−24 mm; −59 mm) indicating more river runoff than incoming precipitation and consequently water inflow into the system. Figure 8 shows monthly sums for measured runoff and distributed model runoff for summer months of the years 2007 to 2011. Modeled runoff underestimates measured runoff. Figure 9 shows the annual dynamic of main water balance components for each hydrological year within the study period for subbasin Königssetal. Figure 9a,b shows the sum of snowmelt and rain and snowmelt only. In November, snowmelt and rain are hydrological input into the system, from February to June snowmelt is dominant, and from June to October it is mainly rainfall that contributes to the water balance in the subbasin. The evapotranspiration (Fig. 9c) shows an annual dynamic with a peak in July. Figure 9d shows water storage derived from the modeled runoff by the distributed model. In winter months, storage is nearly zero, in spring values are negative due to snow melt, while in summer values are slightly positive due to soil water storage. Figure 9e shows the water storage derived from the measured runoff. In winter months, the storage is positive due to snow cover build-up. In May there is strong snow

melt impact, leading to negative storage values. In summer months, storage remains negative, indicating water inflow through unknown subsurface processes. We assume that underground catchment sizes differ from surface catchment sizes as they are presumed for distributed modeling, and that this is the cause of deviating water storage quantities (Fig. 2).

4 Artificial neural net to calculate boundary fluxes and distributed model correction

Analysis of the mismatches indicate, that there are systematic subsurface boundary fluxes, which can be expressed as observed water storage. The distributed model needs to be adapted to the special hydrological systems in the high Alpine karst environment. We developed an Artificial Neural Network (ANN) as introduced by Herz et al. (1991) and Haykin (1999) to calculate the observed water storage (Fig. 2). Neural networks have already been applied in karstic environments by Dou et al. (1997); Dixon (2005); Siou et al. (2011); Kurtulus and Razack (2010); Kunstmann et al. (2006a) to calculate spring response and stream discharge. The Artificial Neural Network in our study does not calculate stream or spring discharge, but the observed water storage. With this method we describe the strong heterogeneity and discontinuity of the medium. Input variables are distributed model outputs. Artificial Neural Network approaches are usually implemented using libraries, as they are e.g. available for the Matlab® Neural Network Toolbox libraries. We present the analytical solution of the neural network to enable implementation of this method within the distributed model source code.

4.1 Artificial Neural Network (ANN)

We implemented a two layer feedforward Artificial Neural Network (ANN) with a sigmoid function in the hidden layer and a linear function in the output layer for the subbasins Klausbachtal, Wimbachtal and Königsseetal each (Fig. 10). The exogenous inputs are

monthly means of temperature $T_m(t)$, relative humidity $RH_m(t)$ and monthly sums of snowmelt $SN_m(t)$ and rain $P_m(t)$, which is $QS_m(t)$ (Eq. 4) and gives the observed water storage $S(t)$ (Eq. 5). Explanatory variables for the artificial neural net are outputs of the distributed model to ensure that the ANN is not based on any measured data. During the training process and input data testing, three input variables turned out to perform best. Temperature $T_m(t)$ and air humidity $RH_m(t)$ as interpolated meteorological variables to capture seasonality and air moisture; Q_{Sm} is the calculated input into the hydrological system. This study concentrates on monthly sums; therefore, no sliding window is needed. Selection of the number of hidden neurons was done by trial and error. Best results were obtainend with 20 neurons ($n = 20$) in the hidden layer. The ANN was trained and validated with 65 months ($m = 65$) and tested for $m = 44$ (test data). The dataset for training and validation was split up into $m = 56$ (85 %) for training and $m = 11$ for validation (15 %). Net training to obtain the parameters a_i to f_i was done with the Levenberg-Marquardt algorithm for which the RMSE was chosen as the objective function to be minimized (Eq. 6). Table 5 shows the weights and biases derived by the training process.

$$QS_m(t) = P_m(t) + SN_m(t) \tag{4}$$

$$S_{obs_{ANN}}(t) = a_i + \sum_{i=1}^{n} \frac{b_i}{1 + e^{c_i + d_i QS_m(t) + e_i T_m(t) + f_i RH_m(t)}} \tag{5}$$

$$RMSE = \sqrt{\frac{1}{n} \sum_{i=1}^{n} (S_{obs_{ANN}}(t) - S_{obs_{real}}(t))^2} \tag{6}$$

Net input and output were normalized from $r_{min} = -1$ to $r_{max} = 1$ and backtransformed using the following equations (Eqs. 7 and 8) during pre- and postprocessing:

$$y = (r_{max} - r_{min}) \frac{x - x_{min}}{x_{max} - x_{min}} + r_{min} \tag{7}$$

$$x = (y + 1)(x_{max} - x_{min})/2 + x_{min} \tag{8}$$

Performance evaluation – ANN

We show monthly sums of observed water storage simulated with the ANN in subbasin Königsseetal for the test period of the neural net from March 2007 to October 2009 ($m = 444$). Correlation of the observed water storage simulated with the ANN and the observed water storage give $r^2 = 0.48$ (Fig. 11), whereby the NSE = 0.43 and the RMSE = 0.27 (Table 6). Figure 12a represents modeled water storage based on the distributed model and observed water storage from June 2007 to October 2009 ($n = 44$), showing deviations during summer months. The distributed model underestimates river runoff in the given subbasin from April to October 2007, from June to September 2008 and from June to October 2009. Underestimation also occurs during the summer months when snow melt is not present. Figure 12b represents water storage by the distributed model and observed water storage and the observed water storage simulated with the ANN. The ANN is able to represent observed water storage during summer months. It underestimates observed water storage in November 2007 and Mai 2009 and it overestimates water storage in June 2009. The observed water storage simulated with the ANN is then implemented in the distributed model as a constant boundary flux to improve distributed model within that time period.

4.2 Distributed model correction: implementation of boundary flux in the saturated zone

We used the monthly outcomes of the artificial neural network as a basis for the constant boundary flux into the distributed model (Fig. 2). The monthly sum of observed water storage simulated with the neural net was subtracted from the modeled water storage already calculated for the investigated period (Eq. 9). The difference was implemented as continuous boundary flux $Q_{\text{bound}}(t)$ in $\text{m}\,\text{s}^{-1}$ per hour for each month in the saturated zone at selected sites at the border of subcatchments. Therefore, the hydrological model was constantly corrected during model run. The correction was

subsequently considered in consecutive modules of the distributed model and finally routed to river outlets.

$$Q_{\text{bound}}(t) = S_{\text{mod}}(t) - S_{\text{obs}_{\text{ANN}}}(t) \tag{9}$$

This method is not a bias correction of modeled runoff at the outlet point, but an inflow within the groundwater model, which the model accounts for and which is considered in the following modeling process. The inflow size can vary from one grid cell to the whole subbasin area. We implemented a boundary flux based on the results of the test period of the neural net from July to October for the years 2007 to 2009. The results are presented in Fig. 13.

5 Results and discussion

Within the scope of this study, we could show the limitations of a distributed model in high alpine terrain with massive carbonate aquifers. We were able to quantify systematic model mismatch at subbasin scale and point out hydrological processes within these heterogeneous catchments that deviate from common model assumptions (Darcy Flow, Porous Media Conditions). To enable distributed modeling within these catchments, which are the origin of lowland river runoff quantities and dynamics, we developed a method to describe and account for the missing water quantities. By the given station data and interpolation method, unrealistic precipitation assumptions are not the case and could be suspended as the underlying reason for the model mismatch. Therefore, we concluded an uneven observed water balance for the given sub-catchments to be the cause, because of unknown subsurface boundary fluxes. Or, in other words, the real catchment size for river gauges differs from the size assumed by the distributed model due to underground fluxes. By assuming porous conditions, the model is unable to account for extreme differences in hydrological system at catchment scale resulting in consistent model mismatch. Figure 15 shows the results of the distributed model for the hydrological year 2006–2007. It is evident that the grid-based

approach provides detailed information on the heterogeneous Alpine catchment. The annual sum of precipitation ranges from 1300 mm in the valleys to over 2100 mm in mountainous regions. Evapotranspiration is calculated from zero to over 1400 mm at extreme locations. Relative humidity ranges from 0.70 % to over 0.82 %. Mean annual temperature is from 10 °C in valleys to −2 °C at elevated regions. The massive karst aquifer itself and, the location of all conduits and subsurface flow channels, remains a black box. However, based on tracer experiments and the spring locations we were able to synthesize that the main underground flow direction tends to be north, which corresponds with the results of the distributed model mismatch (Kraller et al., 2011). Since we are unable to quantify each underground flux in the study area, and especially the dynamics throughout a hydrological year, we chose a statistical method to capture unknown underground flow processes at catchment scale on a monthly basis. By developing the artificial neural net, we were able to reproduce monthly storage deviations. A two layer feedforward backpropagation network with a sigmoid function in the hidden layer and a linear function in the output layer with 20 neurons in the hidden layer gave best results. The neural net is satisfactory representing observed water storage. We implemented a constant boundary flux in $m\,s^{-1}$ per time step of one hour for each month in the saturated zone module of the distributed model for subbasin Königsseetal from July to October for the years 2007 to 2009 based on the results of the ANN. The influx was then involved in the consecutive modules during model run. Performance of the distributed model improved with implementation of the constant boundary flux (Eq. 9). NSE increased from 0.34 to 0.57 and the RMSE decreased from 6.10 mm to 1.66 mm, which shows that after implementation of the boundary flux the distributed model was better at reproducing the measured runoff (Table 6). Figure 13 shows monthly sums of measured runoff, modeled runoff and modeled runoff after implementing the boundary flux for 2007 to 2009. Measured runoff is improved in most months. In June 2008 and July 2009 the influx did not improve model results. In September 2007, the neural net did not give satisfactory representation of observed storage. Consequently, monthly sums of modeled runoff do

not perfectly match monthly sums of measured runoff after implementing the boundary flux. Figure 14 shows main components of the annual water balance of 2007 in subbasin Königsseetal before and after distributed model correction. As the inflow takes place in the saturated zone module, annual sums of precipitation (1604 mm), evapotranspiration (432 mm), effective precipitation (1181 mm) and observed water storage (−618 mm) are equally calculated before and after the boundary influx. Observed water storage was negative in the annual balance, because subsurface water inflow takes place throughout subbasin borders (derived by the DEM). In the original model run, the modeled runoff (1094 mm) underestimated measured runoff. After implementing the boundary flux, modeled runoff is increased to 1487 mm. Originally, modeled water storage was minimal (18 mm), because the distributed model calculates even annual water balances internally. By correcting the distributed model with the constant inflow on a monthly basis, annual modeled water storage resulted in −306 mm and better reproduction of observed water storage. At river gauge St. Leonhardt, which is the outlet of the whole catchment, modeled runoff also increases, showing improved distributed modeling for the overall study area. Figure 15 shows the mean groundwater level in the region in the year 2006–2007. Based on the assumed soil layers, which had to be in the given range of the distributed model, groundwater reaches the surface in valley regions, as steep gradients lead to increased flow in hill slopes. Soil moisture in the root zone ranges from zero to almost 100 %. Storage capacities are reached within the saturated zone in the given soil layers, and water excess is given to the unsaturated zone. Figure 16 presents runoff components of modeled runoff in year 2007 before and after implementation of the boundary flux. In the original model run, interflow and baseflow were calculated almost equally, whereas direct flow is the main contributor to modeled runoff. After implementing the boundary flux, interflow increased most, whereas baseflow and directflow remain almost unchanged. As the groundwater module and unsaturated zone module in the distributed model are coupled bidirectionally, baseflow is converted to interflow within model performance. ANN has been used previously in hydrological studies, but mainly to predict and calculate

the discharge of a given river course or spring rather than deviating storage conditions. Our new method describes the ANN analytically, and enables to calculate unknown storage processes in complex hydrogeological environments on a monthly basis. With this method, the distributed model reproduces storage conditions more realistically in high Alpine karst terrain, which leads to a more realistic runoff at catchment scale.

6 Summary and conclusions

We implemented a distributed water balance model in the watershed of the river Berchtesgadener Ache. The model area was derived during preprocessing by surface water divides. Since the model area is situated in high Alpine karst, we expect groundwater basins sizes to differ from surface basin sizes. This was also indicated by Kraller et al. (2011), who synthesized northerly subsurface water flow direction. Subsurface water fluxes in the unsaturated zone and saturated zone lead to an uneven water balance. Each of the three neighbouring high Alpine head sub-catchments is unique in its hydrology. Distributed modeling resulted in systematic model mismatch in the high alpine neighboring subbasins. Model mismatch is a consequence of water storage deviations in reality and the distributed model. To improve the distributed model in high Alpine karst dominated catchments, we developed an artificial neural net to calculate missing fluxes in monthly sums that can then be implemented as inflow or outflow in the saturated zone of the distributed model. The results obtained with the artificial neural net respresent observed water storage satisfactorily. Implementation of missing boundary fluxes in the distributed model improved modeled runoff at subbasin scale. Further studies will show that the approach can be generalized on a larger spacial scale.

Acknowledgements. This project was initiated and financed by the Authority of the Berchtesgaden National Park. The authors gratefully acknowledge the continuous support of Michael Vogel, head of the Berchtesgaden National Park and Helmut Franz, research coordinator of the Berchtesgaden Nationalpark. Furthermore we want to thank Günther Kus for helpful comments. Special thanks go to involved institutes and authorities for data supply and to Severin Kaspar for motivated neural network discussions. We also thank the European Environment Agency (EEA) for providing Corine Land Cover Data (CLC) for land use classification.

References

Attkinson, T.: Diffuse flow and conduit flow in limestone terrain in the Mendip Hills, Sommerset (Great Britain), J. Hydrol., 35, 93–110, 1977. 217

Bakalowicz, M.: Karst groundwater: a challenge for new resources, Hydrogeol. J., 13, 148–160, 2005. 217

Barthel, R.: A indicator approach to assessing and predicting the quantitative state of groundwater bodies on the regional scale with a special focus on the impacts of climate change, Hydrogeol. J., 19, 525–546, 2011. 218

BGRSGD: HUEK200, Hydrogeologische Übersichtskarte von Deutschland, Oberer Grundwasserleiter, Tech. rep., Bundesanstalt für Geowissenschaften und Rohstoffe, Staatliche Geologische Dienste der BRD, 2007. 223

Birk, S., Liedl, R., and M, S.: Identification of localised recharge and donuit flow by combined analysis of hydraulic and physico-chemical spring responses (Urenbrunnen, SW Germany), J. Hydrol., 286, 179–193, 2004. 217

Bonacci, O.: Karst springs hydrographs as indicators of karst aquifers., Hydrolog. Sci. J., 38, 2/1993, 51–62, 2004. 217

Brutsaert, W.: Evaporation into the Atmosphere, Kluwer Academic Publishers, 1982. 222

Caroll, R., Pohll, G., Earman, S., and Hershey, R.: A comparison of groundwater fluxes computed with MODFLOW and a mixing model using deuterium: application to the eastern Nevada Test Site and vicinity, J. Hydrol., 361, 371–385, 2008. 218

Dixon, B.: Application of neuro-fuzzy techniques in predicting ground-water vulnerability: a GIS-based sensitivity analysis, J. Hydrol., 309, 17–38, 2005. 227

Dou, C., Wold, W., Dahab, M., and Bogardi, I.: Transient ground-water flow simulation using a fuzzy set approach, Ground Water, 35, 205–215, 1997. 227
EEA: Regional climate change and adaption, The Alps facing the challenge of changing water resources, EEA Report, No. 8/2009, Tech. rep., EEA, 2007. 217
Einsiedl, F.: Flow system dynamics and water storage of a fissured-porous karst aquifer characterized by artificial and environmental tracers, J. Hydrol., 312, 312–321, 2005. 217
Fischer, K.: Geomorphologie der Berchtesgadener Alpen – Forschungsbericht 50, Nationalparkverwaltung Berchtesgaden, 2005. 220
Ford, D.: Perspectives in karst hydrogeology and cavern genesis, Speleogenesis and Evolution of Karst Aquifers, 1, 3, 2003. 217
Geyer, T., Birk, S., Liedl, R., and Sauter, M.: Quantification of temporal distribution of recharge in karst systems from spring hydrographs, J. Hydrol., 348, 452–463, 2008. 217
Goldscheider, N.: Alpine Hydrogeologie, Grundwasser – Zeitschrift der Fachsektion Hydrogeologie, 16, 2011. 217
Grasso, D. and Jeannin, P.-Y.: A global experimental system approach of karst springs' hydrographs and chemographs, Ground Water, 40, 608–617, 2002. 217
Hauns, M., Jeannin, P.-Y., and Atteia, O.: Dispersion, retardation and scale effect in tracer breakthrough curves in karst conduits, J. Hydrol., 241, 177–193, 2001. 217
Haykin, S.: A Comprehensive Foundation, Macmillan New York, 1999. 227
Herz, J., Krough, A., and Palmer, R.: Introduction to the Theory of Neural Computation, Addison-Wesley, Reading, MA, 1991. 227
Jansson, P. and Karlberg, L.: Coupled heat and mass transfer model for soil-plant-atmosphere systems, Tech. rep., available at: ftp://www.lwr.kth.se/CoupModel.pdf, Royal Institute of Technology, Dept of Civil and Environmental Engineering, Stockholm, 2001. 223
Kiraly, L.: Karstification and Groundwater Flow, Speleo, 1, 155–190, 2003. 217, 218
Kovacs, A., Perrochet, P., Kiraly, L., and Jeannin, P.-Y.: A quantitative method for the characterisation of karst aquifers based on spring hydrographs analysis, J. Hydrol., 303, 152–164, 2001. 217
Kraller, G., Strasser, U., and Franz, H.: Effect of Alpine karst on the hydrology of the Berchtesgadener Ache basin: a comprehensive summary of karst research in the Berchtesgaden Alps, eco.mont., 3, 19–28, 2011. 219, 221, 231, 233
Kunstmann, H., Heckl, A., and Rimmer, A.: Physically based distributed hydrological modelling of the Upper Jordan catchment and investigation of effective model equations, Adv. Geosci.,

9, 123–130, doi:10.5194/adgeo-9-123-2006, 2006a. 223, 227
Kunstmann, H., Krause, J., and Mayr, S.: Inverse distributed hydrological modelling of Alpine catchments, Hydrol. Earth Syst. Sci., 10, 395–412, doi:10.5194/hess-10-395-2006, 2006b. 218
Kurtulus, B. and Razack, M.: Modeling daily discharge responses of a large karstic aquifer using soft computing methods: Artifical neural network and neuro-fuzzy, J. Hydrol., 381, 101–111, 2010. 227
Langenscheidt, E.: Die Geologie der Berchtesgadener Berge, Berchtesgadener Anzeiger, 1994. 220
Lotz, A.: Alpine Habitat Diversity – HABITALP – Project Report 2002–2006, EU Community Initiative INTERREG III B, Alpine Space Programme, Tech. rep., Nationalpark Berchtesgaden, 2006. 223
Maloszweski, P., Buettner, G., Apel, R., Krafft, H., Scholz, M., and Wagner, B.: Quantitative evaluation of tracer experiments in Alpine Karst and Porous Aquifers in the National Park of Berchtesgaden, Lands, 48, 11–18, 2005. 217
Martinez Santos, P. and Andreu, J.: Lumped and distributed approaches to model natural recharge in semiarid karst aquifers, J. Hydrol., 388, 389–398, 2010. 218
Monteith, J.: Vegetation and the Atmosphere, vol. 1: Principles, Academic Press, London, 1975. 222
Penman, H.-L.: Natural evaporation from open water, bar soils and grass, P. ROY. Soc. Lond. A, 191–205, 1948. 222
Peschke, G.: Ein zweistufiges Modell der Infiltration von Regen in geschichtete Böden, Acta Hydrophys., 22, 39–48, 1977. 222
Richards, L.: Capillary conduction of liquids through porous mediums, Physics, 1, 318–333, 1931. 222
Rimmer, A. and Salingar, Y.: Modelling precipitation-streamflow processes in karst basin: The case of the Jordan River sources, Israel, J. Hydrol., 331, 524–542, 2006. 218
Romanov, D., Gabrovsek, F., and Dreybrodt, W.: Modeling the evolution of karst aquifers and speleogenesis, The Step from 1-dimensional to 2-dimensional modeling domains, Speleogenesis and Evolution of Karst Aquifers, 2, 2004. 217
Sauter, M., Kovacs, A., Geyer, T., and Teutsch, G.: Modellierung der Hydraulik von Karstgrundwasserleitern – Eine Übersicht, Grundwasser, 3, 143–156, 2006. 217

Scanlon, B., Mace, R., Barret, M., and Smith, B.: Can we simulate regional groundwater flow in a karst system using equivalent porous media models? Case study, Barton Srpings Edwards aquifer, USA, J. Hydrol., 276, 137–158, 2003. 218

Schulla, J.: Hydrologische Modellierung von Flussgebieten zur Abschätzung von Folgen von Klimaänderungen – Diss ETH 12018, Ph.D. thesis, Geographisches Institut ETH Zürich, 1997. 222, 223

Schulla, J.: Model Description WaSiM-ETH, Tech. rep., ETH Zürich, 2007. 222, 223

Siou, L., Johannet, A., Borrel, V., and Pistre, S.: Complexity selection of a neural network for karst flood forecasting: the case of the Lez Basin (Southern France), J. Hydrol., 403, 367–380, 2011. 227

Strasser, U.: Modelling of the mountain snow cover in the Berchtesgaden National Park, Forschungsbericht 55, Nationalparkverwaltung Berchtesgaden (Hrsg.), Berchtesgaden, 2008. 222

Teutsch, G. and Sauter, M.: Groundwater modeling in karst terrains: scale effects, dam acquisition and field validation, 34d Conference on hydrogeology, ecology, monitoring and management of ground water in karst terranes, Nashville, USA, 17–35, 1991. 217

Van Genuchten, M.: Zur Messung und Schätzung der potentiellen Verdunstung, Z. Meteorol., 25, 103–111, 1976. 222

Viviroli, D. and Weingartner, R.: The hydrological significance of mountains: from regional to global scale, Hydrol. Earth Syst. Sci., 8, 1017–1030, doi:10.5194/hess-8-1017-2004, 2004. 217

Weiler, M., McGlynn, B., Kevin, M., and McDonnell, J.: How does rainfall become runoff? A combined tracer and runoff transfer function approach, Water Resour. Res., 39, 1315–1327, 2003. 217

White, W.: Karst hydrology: recent developements and open questions, Eng. Geol., 65, 85–105, 2002. 217

White, W.: Conceptual models for karstic aquifers, Speleogenesis and Evolution of Karst Aquifers, 1, 3, 2003. 217

White, W. and White, E.: Conduit fragmentation, cave patterns and the localization of karst groundwater basins: the Appalachians as a test case, Speleogen. Evol. Karst Aquif., 1, 1–15, 2003. 218

Worthington, S.: A comprehensive strategy for understanding flow in carbonate aquifer, Speleogenesis and Evolution of Karst Aquifers, 1, 2003. 218

Table 1. Location, altitute and parameters and temporal resolution of the meteorological stations used for our investigation (T = air temperature, H = relative humidity, WS = wind speed, SD = snow depth, SWE = snow water equivalent, SS = sunshine duration, GR = global radiation, DR = direct radiation, RR = relfelcted radiation, P = precipitation, AP = atmospheric pressure at sea level, TS = surface temperature, LWZ = Bavarian avalanche warning service, NPV = Administration Berchtesgaden National Park, ZAMG = Central Institute for Meteorology and Geodynamics Austria).

Station	Altitude [m a.s.l.]	Parameters	Temporal resolution	Operator
Reiteralm1	1755	*T*, *H*, WS, WD	10 min	LWZ
Reiteralm2	1670	*T*, *H*, TS, SD	10 min	LWZ
Reiteralm3	1615	*T*, *H*, *P*, GR RR, SD	10 min	LWZ
Schönau	617	*T*, *H*, *P*, GR, DR, SS, WS, WD, AP	10 min	Schönau/NPV/DWD
Jenner	1200	*T*, *H*, *P*, WS, TS, SD	10 min	LWZ
Höllgraben	653	*T*, *H*, P	10 min	LWZ
Kühroint	1407	*T*, *H*, *P*, WS, WD, GR, RR, TS, SD, SWE	10 min	LWZ
Funtenseetauern	2445	*T*, *H*, WS,WD	10 min	LWZ
Lofer	625	*T*, *P*, *H*, WS, WD, GR, SS, AP	1 h	ZAMG
Loferer Alm	1623	*T*, *P*, *H*, WS, WD, GR, SS, AP	1 h	ZAMG
SBG Flughafen	430	*T*, *P*, *H*, WS, WD, GR, SS, AP	1 h	ZAMG
Schmittenhöhe	1973	*T*, *P*, *H*, WS, WD, GR, SS, AP	1 h	ZAMG
Königsberg Pegel	699	*P*	1 d	NPV
Schapbach	953	*P*	1 d	NPV
Kühroint (mech.)	1418	*P*	1 d	NPV
Lahneralm	1240	*P*	1 d	NPV
St. Bartholomä	604	P	1 d	NPV
Wimbachschloss	926	*P*	1 d	NPV
Brunftbergtiefe (mech.)	1238	*P*	1 d	NPV
Auf dem Gries	1435	*P*	1 d	NPV
Bindalm	1119	*P*	1 d	NPV
Eckau	1015	*P*	1 d	NPV
Lahnwaldfütterung	840	*P*	1 d	NPV
Mittereis	1325	*P*	1 d	NPV
Halsalm	1088	*P*	1 d	NPV

Table 2. Precipitation interpolation analysis. Inverse Distance Weighting (IDW), Regression (REG) and the combination of Regression and IDW (REG + IDW) in the year 2006/2007 for subbasin Königsseetal (4). Regression and REG + IDW for station location (Kühroint) – mean 2001–2010.

Scale	Time period	IDW [mm]	REG [mm]	REG + IDW [mm]	Station Data (Kühroint) [mm] (1407 m a.s.l.)
Subbasin	Sum 2006/2007	1559	1704	1643	–
Station	Mean 2001–2010	–	1468	1670	1676

Table 3. Annual sums and mean of precipitation, evapotranspiration, modeled and measured discharge – subbasins Klausbachtal, Wimbachtal and Königsseetal

	Year	Klausbachtal	Wimbachtal	Königsseetal
Area [km^2]		42.79	35.69	163.54
Precipitation/evapotranspiration [mm]	2001/2002	2112/349	1940/354	1869/446
	2002/2003	1652/405	1533/393	1469/477
	2003/2004	1782/355	1718/351	1639/420
	2004/2005	1832/338	1745/319	1655/371
	2005/2006	1607/331	1574/310	1511/362
	2006/2007	1672/355	1621/355	1604/423
	2007/2008	1739/389	1654/353	1774/465
	2008/2009	1818/192	1899/350	1804/434
	2009/2010	1739/389	1654/353	1774/435
Mean precipitation/evapotranspiration [mm]		1772/367	1704/348	1681/425
Measured/modeled runoff [mm]	2001/2002	1183/1541	1535/1411	1402/1297
	2002/2003	1375/1260	1872/1146	1634/1002
	2003/2004	996/1371	1045/1265	1197/1178
	2004/2005	1253/1450	1783/1351	1596/1241
	2005/2006	1235/1291	2622/1255	1784/1137
	2006/2007	1259/1175	2269/1175	1799/1094
	2007/2008	1128/1283	2346/1226	1831/1291
	2008/2009	1178/1178	2544/1335	1597/1240
	2009/2010	1253/1282	2808/1353	1593/1332
Mean measured/modeled runoff [mm]		1207/1325	2091/1280	1604/1201

Table 4. Minimum, maximum and mean of monthly modeled (S_{mod}) water storage by the distributed model and observed water storage (S_{obs}) in subbasin Klausbachtal, Wimbachtal and Königsseetal (mm)

	Klausbachtal $S_{mod}/S_{obs_{real}}$	Wimbachtal $S_{mod}/S_{obs_{real}}$	Königsseetal $S_{mod}/S_{obs_{real}}$
Max	264/271	275/207	285/439
Min	−282/−199	−282/−328	−366/−349
Mean	−2/15	5/−21	1/−59

Table 5. Weights and biases ANN. b_i = weight hidden layer to output. d_i, e_i, f_i = weights layer 1 to hidden layer. c_i = bias layer 1 to hidden layer. a_i = −0.54 (bias hidden layer to output).

b_i	c_i	d_i	e_i	f_i
−0.35	4.99	−8.50	4.96	2.44
0.13	2.37	−11.70	2.143	1.398
−1.07	4.53	−6.87	−2.25	5.19
−1.6	−1.65	9.21	−2.32	−4.00
−0.04	−3.07	2.71	−6.02	−5.72
0.23	0.71	−3.88	−5.79	−5.12
0.82	0.06	−6.16	−3.36	−5.49
−0.17	0.68	−4.06	−7.77	1.60
0.84	0.78	9.94	3.65	3.76
0.56	3.55	9.29	−3.49	0.52
−0.05	0.63	1.00	−1.21	−7.14
0.17	−0.01	1.85	−5.75	−8.72
0.03	4.38	4.47	5.75	4.38
0.74	−3.53	−11.77	0.54	1.70
0.06	5.15	3.12	7.94	1.10
0.37	−9.02	−8.6	1.46	−3.33
−1.65	−6.59	−2.00	5.99	3.69
1.57	−4.92	−1.70	5.67	3.38
0.01	−10.03	−10.03	−3.00	2.02
−0.13	12.27	−10.26	3.30	−2.02

Table 6. Performance evaluation Artificial Neural Net (observed water storage and modeled water storage) and distributed model correction (measured vs. modeled discharge).

Efficiency criteria	ANN	Distributed modeling without ANN extention	Distributed modeling with ANN extention
Coefficient of Determination (r^2)	0.48	0.80	0.79
Coefficient of Efficiency (NSE)	0.43	0.34	0.57
Root Mean Square Error (RSME) [mm]	0.27	6.10	1.66

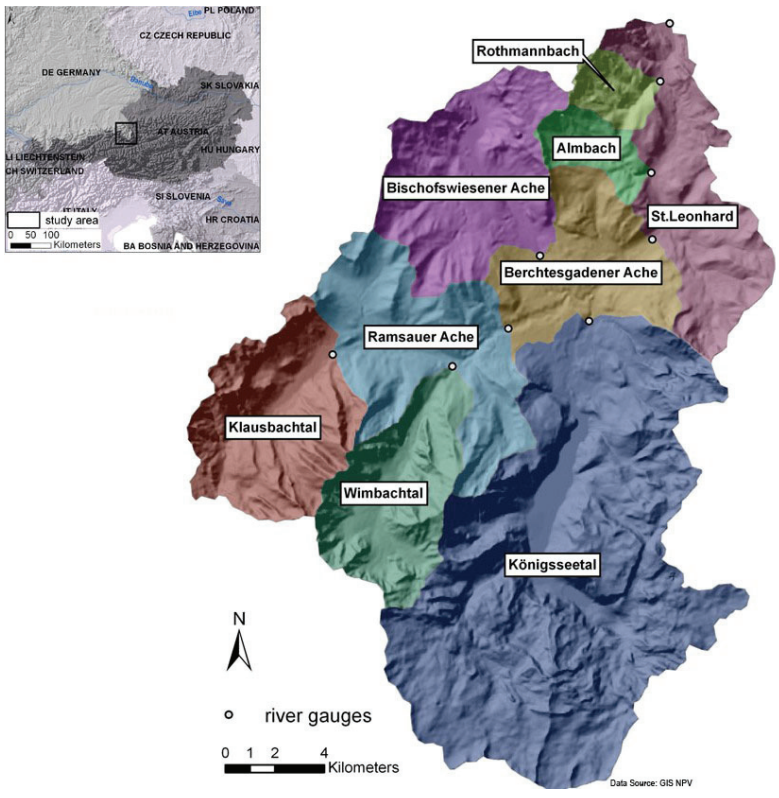

Fig. 1. Study area: river gauges and subbasins.

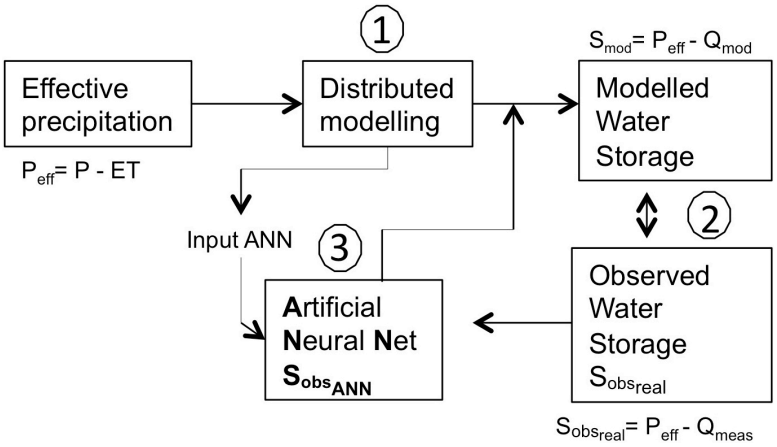

Fig. 2. Overview of the presented method. Effective precipitation (Precipitation *P* minus Evapotranspiration ET) results in modeled runoff Consistent model mismatch was detected due to water storage deviations. Modeled water storage (derived from distributed model runoff) systematically over/underestimates observed water storage (derived from measured runoff). The observed water storage is then calcualted by the ANN and implemented in the groundwater module to account for the observed storage processes.

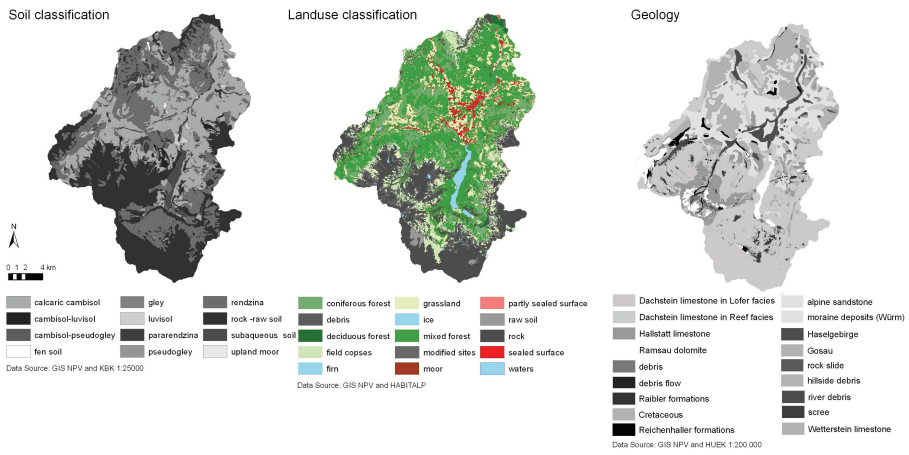

Fig. 3. Soil classification, landuse classification and main geological units within the study area.

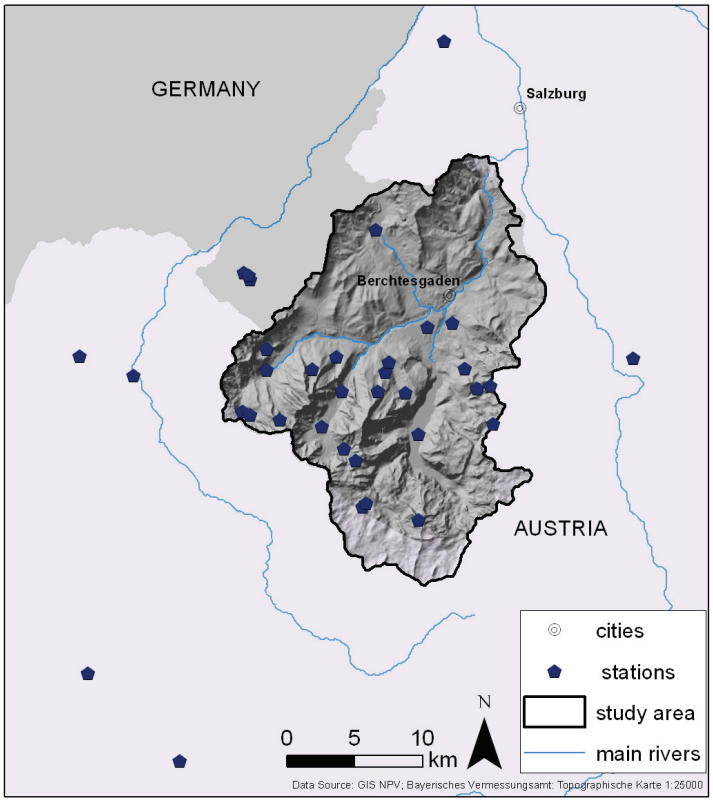

Fig. 4. Locations of weather stations within and outside the study area.

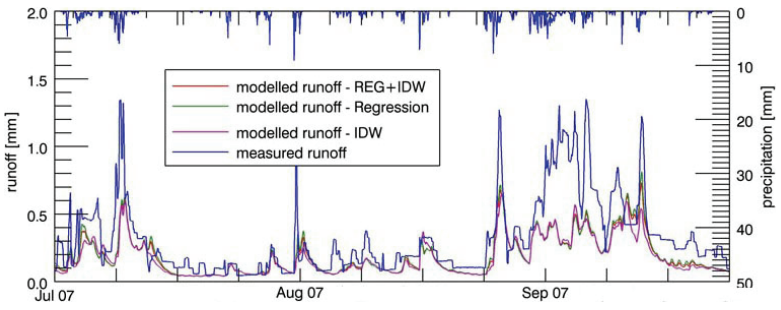

Fig. 5. Comparison of different interpolation methods in subbasin Königsseetal. Inverse Distance Weighting (IDW), Elevation dependent Regression (REG) and both methods linearly combined (IDW + REG).

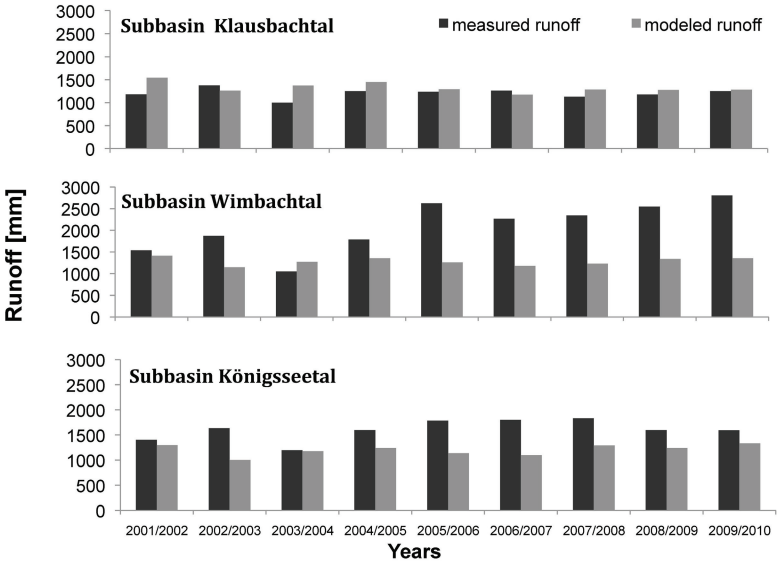

Fig. 6. Annual sums of modeled and measured discharge subbasins Klausbachtal, Wimbachtal and Königsseetal.

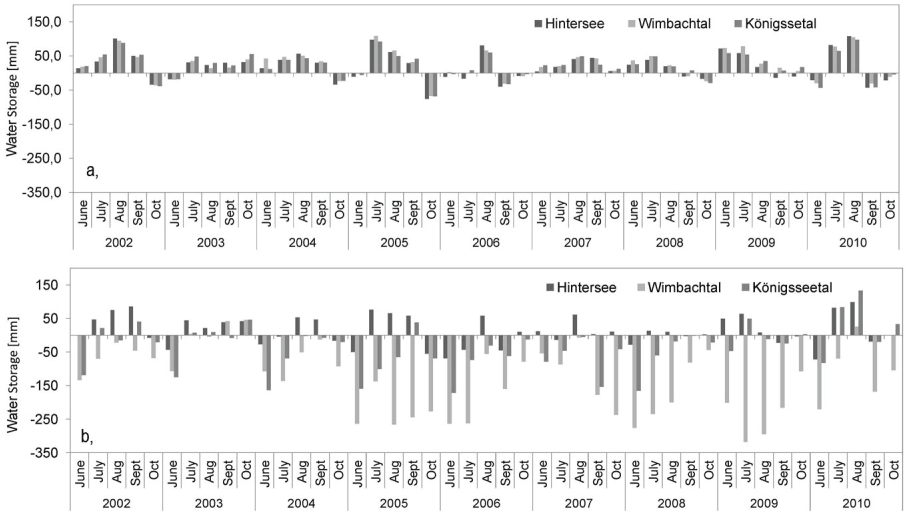

Fig. 7. **(a)** Comparison of the water storage (S_{mod}) derived from results of distributed model runoff. Monthly sums July–October 2001–2011 – subbasins Klausbachtal, Wimbachtal, Königsseetal. **(b)** Comparison of the water storage ($S_{obs_{real}}$) derived from measured runoff. Monthly sums July–October 2001–2011 – subbasins Klausbachtal, Wimbachtal, Königsseetal.

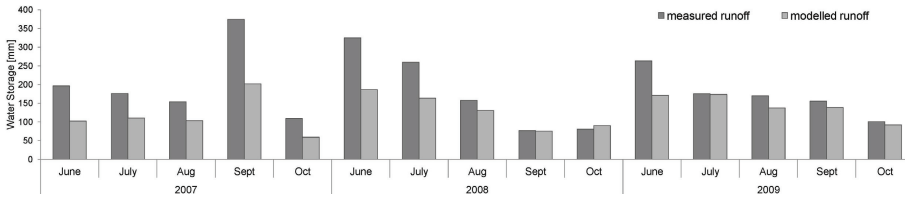

Fig. 8. Monthly sums of measured runoff and modeled runoff in subbasin Königsseetal – June to October for years 2007 to 2009.

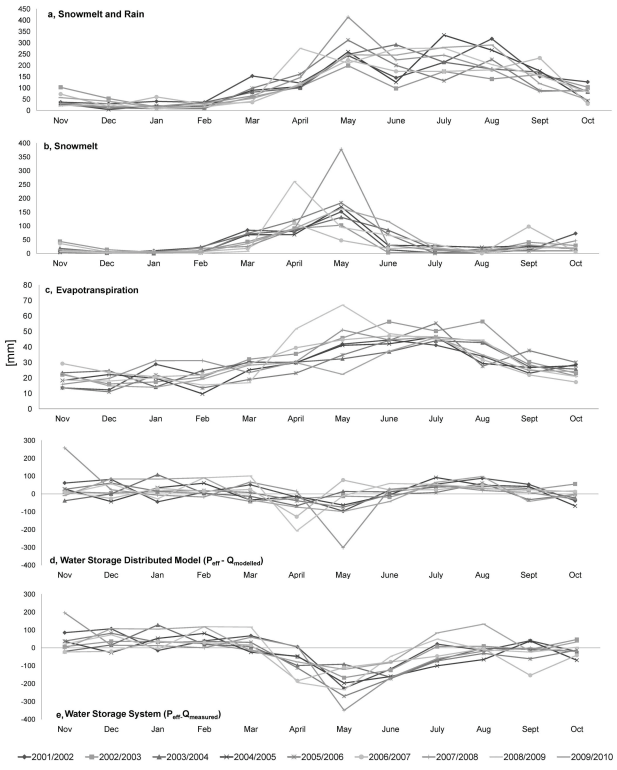

Fig. 9. Monthly sums of snowmelt + rain **(a)**, snowmelt **(b)**, evapotranspiration **(c)**, water storage distributed model **(d)** and observed water storage **(e)** for hydrological years 2001–2010 in subbasin Königsseetal.

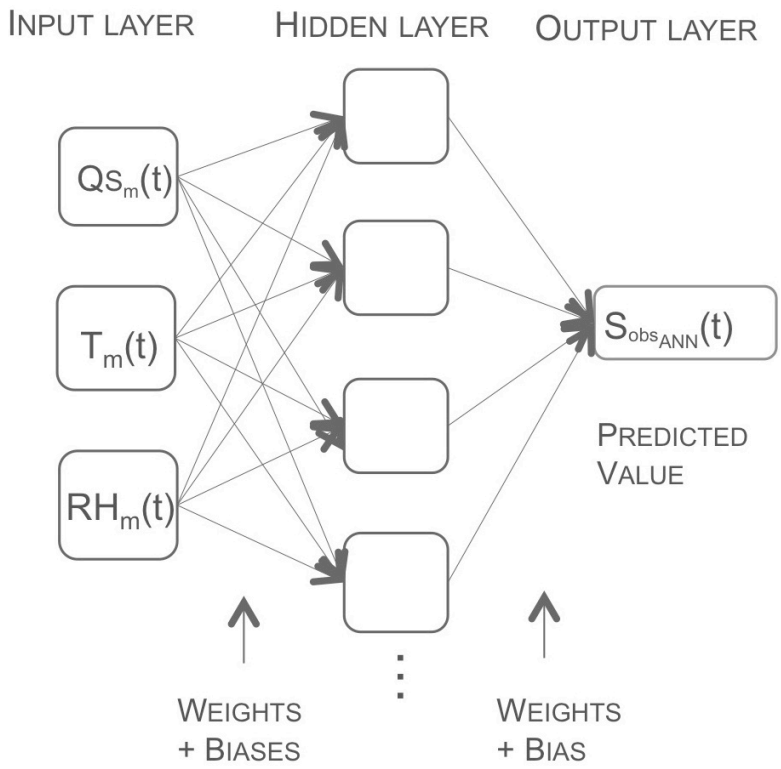

Fig. 10. Architecture Artificial Neural network. Input Layer, Hidden Layer and Output Layer.

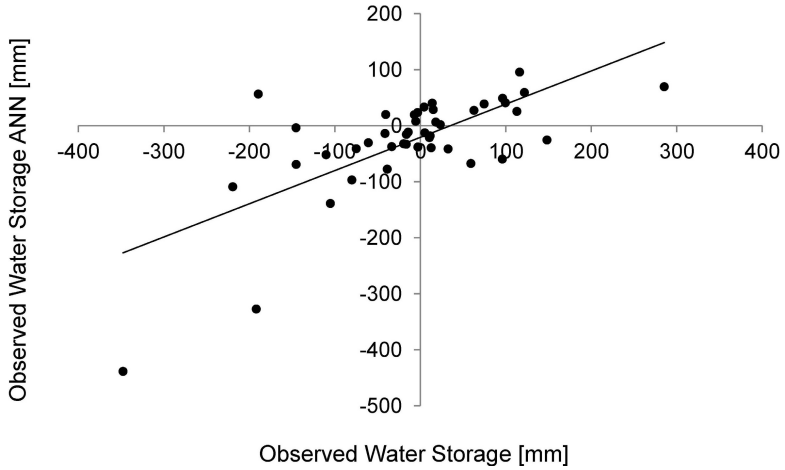

Fig. 11. Performance ANN – Test period. Correlation diagram between simulated monthly observed water storage by the ANN vs. observed water storages.

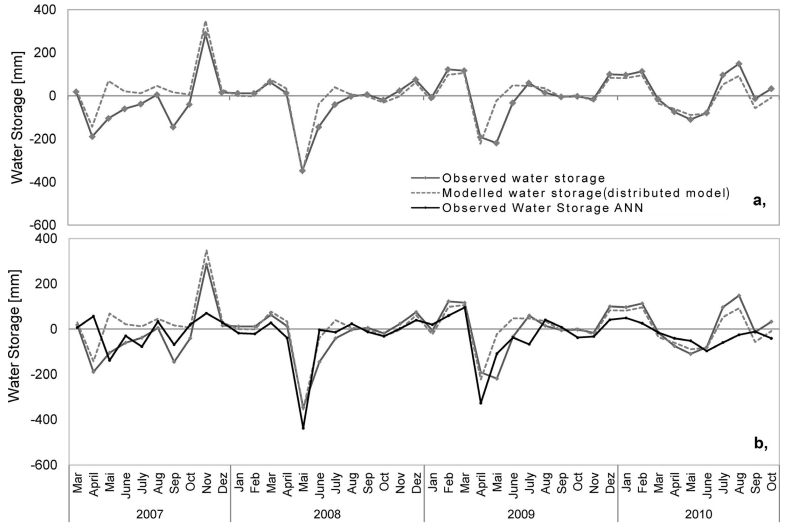

Fig. 12. Comparison of observed water storage and observed water storage simulated by the ANN in monthly sums. Test period of the neural net in subbasin Königsseetal. The upper graph shows the observed water storage and the water storage by the distributed model. The lower diagram is showing the simulated observed water storage by the artificial neural network.

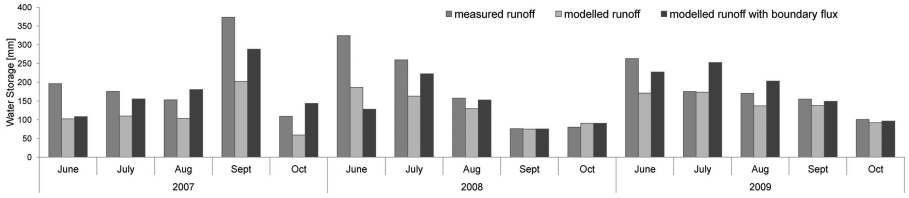

Fig. 13. Monthly sums of measured runoff and distributed model runoff with and without implemented boundary flux from June to October for years 2007–2009 – subbasin Königsseetal.

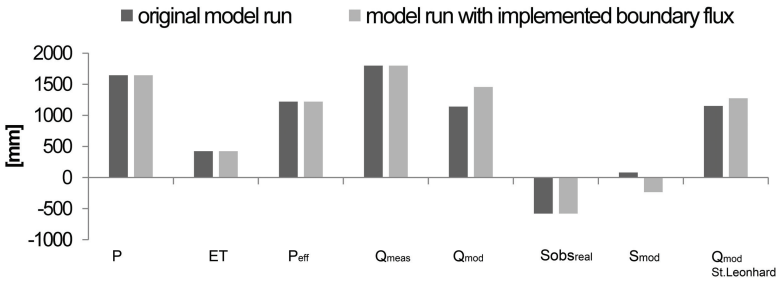

Fig. 14. Water balance components for subbasin Königsseetal and modeled runoff for St. Leonhard – annual sums 2007. Results for original model run and model run with implemented boundary flux (P = Precipitation, ET = Evapotranspiration; P_{eff} = effective precipitation, Q_{obs} = measured runoff, Q_{mod} = modeled runoff, S_{obs} = observed storage, S_{mod} = modeled storage).

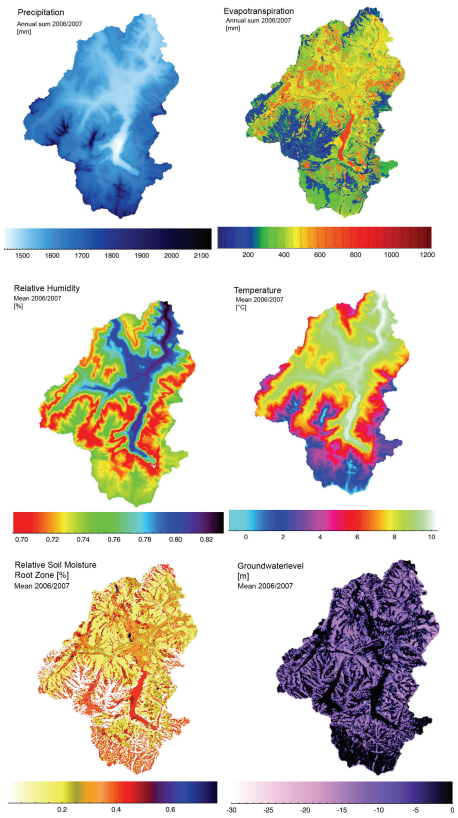

Fig. 15. Spatial water balance results of the distributed model. Precipitation and Evapotranspiration, Relative Humidity, Temperature, Groundwaterlevel and Relative Soil Moisture.

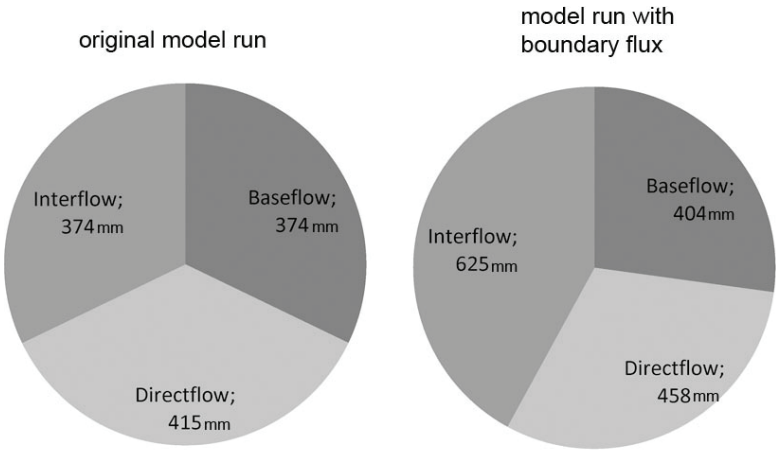

Fig. 16. Components of modeled runoff. Subbasin Königsseetal – annual sums [mm] 2007. Results for original model run and model run with implemented boundary flux.